



## Correlations between black carbon mass and size-resolved particle number concentrations in the Taipei urban area: A five-year long-term observation

Yu-Hsiang Cheng<sup>1</sup>, Yu-Yun Kao<sup>1</sup>, Jyh-Jian Liu<sup>2</sup>

<sup>1</sup> Department of Safety, Health and Environmental Engineering, Ming Chi University of Technology, 84 Gungjuan Rd, Taishan, New Taipei 24301, Taiwan

<sup>2</sup> Department of Environmental Monitoring and Information Management, Environmental Protection Administration, 83, Sec. 1, Zhonghua Rd, Zhongzheng, Taipei 10042, Taiwan

### ABSTRACT

This study investigates the correlation between Black Carbon (BC) mass and particle number concentrations in various particle size ranges in Taipei urban area. The concentrations of BC mass and particle numbers (ranging from 10–560 nm,  $N_{10-560}$ ) were measured continuously from 2006 to 2010. Long-term measurement results of this study demonstrated that BC mass concentrations in the spring, summer, autumn, and winter were  $3.3 \mu\text{g m}^{-3}$ ,  $3.2 \mu\text{g m}^{-3}$ ,  $2.4 \mu\text{g m}^{-3}$ , and  $3.1 \mu\text{g m}^{-3}$ , respectively. Additionally, the  $N_{10-560}$  concentrations in the spring, summer, autumn, and winter were  $1.5 \times 10^4 \text{ particles cm}^{-3}$ ,  $1.7 \times 10^4 \text{ particles cm}^{-3}$ ,  $1.1 \times 10^4 \text{ particles cm}^{-3}$ , and  $1.4 \times 10^4 \text{ particles cm}^{-3}$ , respectively. In the autumn, the lowest BC mass and particle number concentrations were mostly likely owing to the high wind speed condition that favored dispersion of particulate matter. Additionally, the highest particle number concentrations observed in the summer can be due to that the activities of the chemical nucleation reactions in the summer are more intense than those in other seasons. In this sampling site, the number fractions for  $N_{10-18}$ ,  $N_{18-32}$ ,  $N_{32-56}$ ,  $N_{56-100}$ ,  $N_{100-180}$ ,  $N_{180-320}$  and  $N_{320-560}$  were 4.39%, 15.38%, 26.31%, 27.35%, 16.89%, 7.17% and 2.51%, respectively. Hourly BC mass concentrations are significantly positively correlated with hourly  $N_{100-180}$  concentrations at the sampling site. In the summer, a clear increase in  $N_{10-560}/\text{BC}$  is observed during the noontime period, coincident with maximum ambient temperature. Secondary particles through the photochemical nucleation heavily impact the size range of 56–100 nm, following by 100–180 nm and 32–56 nm in this study.

**Keywords:** Black carbon, particle number, photochemical nucleation, Taipei

doi: 10.5094/APR.2014.008



**Corresponding Author:**

*Yu-Hsiang Cheng*

☎ : +886-2-29089899

☎ : +886-2-29084513

✉ : yhcheng@mail.mcut.edu.tw

**Article History:**

Received: 13 August 2013

Revised: 09 October 2013

Accepted: 17 October 2013

### 1. Introduction

Several studies have indicated consistently that exposure to airborne particulate matter may adversely affect public health, particularly respiratory and cardiovascular systems (Duhme et al., 1998; Pope et al., 2004). As an important constituent of aerosols, black carbon (BC) has been identified as significantly contributing to global warming (Schulz et al., 2006; Ramanathan and Carmichael, 2008; Jacobson, 2010; Bond et al., 2013), as well as causing several respiratory diseases and adversely affecting the cardiovascular system (Rich et al., 2005; Jansen et al., 2005; Suglia et al., 2008; Power et al., 2011). In urban environments, BC aerosols are normally generated by incomplete combustion of carbonaceous fuels and are emitted from road traffic and biomass burning (Sandradewi et al., 2008; Fruin et al., 2008; Perez et al., 2010; Snyder et al., 2010; Boogaard et al., 2011; Invernizzi et al., 2011; Rattigan et al., 2013). BC can play a good indicator of combustion sources due to its very low chemical reactivity in the atmosphere. Invernizzi et al. (2011) also suggested that BC is a highly relevant metric of traffic pollution and should be taken into consideration in demonstrating the effectiveness of air quality mitigation measures. Therefore, measurements of BC are important in order to understand the major sources and subsequent evolution in the atmosphere. Long term measurements are of interest in the evaluation of emission control strategies and to assess impacts on health and climate.

Additionally, recent toxicological and epidemiological studies suggest that adverse pulmonary health effects are associated with freshly generated ultrafine particles (Donaldson et al., 2002; Oberdorster et al., 2002), especially ultrafine black carbon particles (Gilmour et al., 2004). Over 80% of airborne particles in urban air are in ultrafine sizes (Hussein et al., 2005; Rodriguez et al., 2007). These ultrafine particles in urban ambient originate from traffic emissions, ranging from  $1.0 \times 10^4$ – $2.0 \times 10^4 \text{ particles cm}^{-3}$  (Hussein et al., 2004; Matson, 2005; Rodriguez et al., 2007; Beckerman et al., 2008; Morawska et al., 2008; Hagler et al., 2009). However, new particles can also be generated from photochemical reactions as secondary pollutants in the atmosphere, particularly under high solar radiation intensity (Rodriguez and Cuevas, 2007; Pey et al., 2009; Cheung et al., 2011). Thus, the major influence on particle number concentrations is vehicle exhaust emissions during the traffic peak hours and new particle formation through photochemical reactions in urban areas.

A lot of information is available about the magnitude of BC mass and particle number concentrations at different environments (Fruin et al., 2008; Boogaard et al., 2011; Reche et al., 2011). Several studies have suggested that exposure to road traffic emissions can be evaluated properly by combining ambient air measurements of BC with particle number concentrations (Harrison et al., 2004; Smargiassi et al., 2005; Rodriguez and Cuevas, 2007). Westerdahl et al. (2005), Rodriguez et al. (2008) and Reche et al. (2011) demonstrated that BC mass concentrations are

positively correlated with total particle number concentrations in urban areas. Cheng et al. (2013) showed that BC mass concentrations at a heavy traffic roadside are significantly positively associated with particle number concentrations ranging from 56–180 nm, indicating most BC in aerosols in urban areas can be in this size range. Kondo et al. (2011) reported that the mass median diameter (MMD) and count median diameter (CMD) of fresh BC aerosols range from 120 to 160 nm and 50 to 80 nm, respectively, in urban areas. However, limited information is available for their correlation between BC mass and particle number concentrations in Taipei urban area, particularly how BC mass and particle number concentrations are related in different particle size ranges.

In this study, BC mass and particle number concentrations were measured simultaneously by using an aethalometer and Scanning Mobility Particle Sizer (SMPS) from 2006 to 2010 at the Taipei Aerosol Supersite. These long-term monitoring results can shed further light on the temporal characteristics of black carbon mass and particle number concentrations in different seasons in Taipei urban area. Moreover, based on the long-term monitoring data, size-fractionated particle number characteristics are elucidated in detail. Exactly how BC mass concentrations and particle number concentrations are related in different particle size ranges was demonstrated as well.

## 2. Methods

### 2.1. Sampling site

Figure 1 shows the location of the Taipei Aerosol Supersite in Northern Taiwan. Taipei Aerosol Supersite is located in a public sports park, which is 5 km west of the Taipei City center. This sports park is approximately 11 000 m<sup>2</sup> and surrounded by a residential and commercial area. This aerosol supersite is located

on the north edge of the park and adjacent to a busy road with a distance of 25 m. On this traffic road, the average traffic flow is approximately 2 000 vehicles per hour during the daytime (Chang et al., 2007). The Taipei Aerosol Supersite monitors ambient aerosols representing typical urban air in northern Taiwan.

### 2.2. Instrumentation

The BC mass concentrations were measured at 880 nm wavelength light with an aethalometer (Magee Model AE31). The particle number size distributions were evaluated using a scanning mobility particle sizer (SMPS; TSI Model 3936). Two primary components of the SMPS are a TSI Model 3080 Electrostatic Classifier which includes a TSI Model 3081 Differential Mobility Analyzer and a TSI Model 3022A Condensation Particle Counter. In this study, SMPS determined particle number concentrations within the range of 10–560 nm in diameter. The sampling inlets of the monitoring instruments were located roughly 4.5 m above ground level. A US EPA-designed PM<sub>10</sub> inlet head was used to sample airborne particulate matter from outside at a sampling flow rate of 16.7 L min<sup>-1</sup>. Inside the monitoring station, a part of the sampled air at the downstream of the PM<sub>10</sub> inlet was drawn through silicone conductive tubing to the monitoring instrument. The monitoring instrument was fixed on a rack which was 1.5 m above ground level. The connecting tubing was approximately 0.5 m in length to keep a lowest inside particle loss. The data logging interval for BC mass and particle number concentrations was set at 5 min. The data in this study were collected continuously from 2006 to 2010. The sampling results can demonstrate the temporal variations of BC mass and particle number concentrations in this urban area. Moreover, hourly averaged wind speed, wind direction, ambient temperature and relative humidity were recorded by a meteorological system at the sampling site.

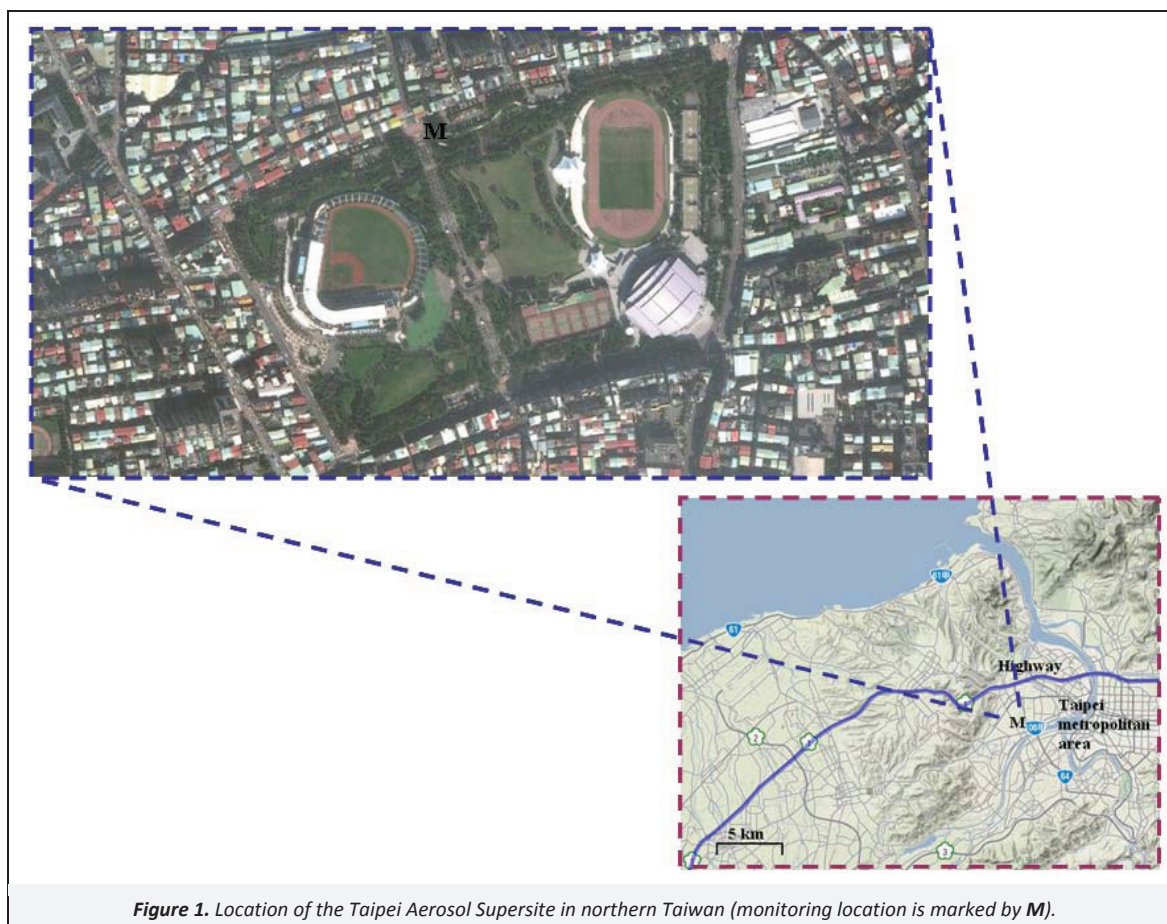


Figure 1. Location of the Taipei Aerosol Supersite in northern Taiwan (monitoring location is marked by M).

### 2.3. Statistical analysis

The hourly particle number ( $N_{10-560}$ ) concentrations within a range of 10–560 nm in size were averaged based on 5 min interval SMPS raw data. The particle number concentrations in 10–18 nm ( $N_{10-18}$ ), 18–32 nm ( $N_{18-32}$ ), 32–56 nm ( $N_{32-56}$ ), 56–100 nm ( $N_{56-100}$ ), 100–180 nm ( $N_{100-180}$ ), 180–320 nm ( $N_{180-320}$ ) and 320–560 nm ( $N_{320-560}$ ) were also determined from SMPS raw data in different size-segregated ranges. Additionally, the mode diameter ( $D_m$ ) of the measured size distribution data by SMPS was evaluated from a log-normal function using DistFit software (Chimera Tech., Inc.). The fitting criterion of  $\chi^2$  was set at 0.02 in this method. The strength of correlations between BC mass and particle number at the sampling site were determined using the Pearson product moment correlation coefficient ( $R_{Pearson}$ ). Furthermore, differences in BC mass (or particle number) concentrations between different monitoring periods were tested using an independent sample *t*-test. Significance was 0.05 for all statistical tests.

## 3. Results and Discussion

### 3.1. Seasonal variations in meteorological conditions at the sampling site

Table 1 summarizes meteorological data throughout the sampling period. Spring, summer, autumn, and winter in Taiwan last from March to May, June to August, September to November, and December to February, respectively. The wind speed in the autumn markedly exceeded those in other seasons (all  $p < 0.001$ ). The lowest mean wind speed was observed in the summer. Figure 2 shows the distributions of hourly wind speed and wind direction in different seasons. Except for the summer, principal wind direction was between east–northeast (ENE) and east–

southeast (ESE). Wind direction between west–northwest (WNW) and west–southwest (WSW) was also observed in the summer. The mean temperatures in the spring, summer, autumn, and winter were 23 °C, 30 °C, 26 °C, and 17 °C, respectively. The temperature in the summer was significantly higher than those in other seasons (all  $p < 0.001$ ). The lowest mean temperature was observed in the winter compared with other seasons. Additionally, the mean relative humidity was approximately 75% and did not differ among all of the seasons.

### 3.2. Seasonal and diurnal variations in BC mass and $N_{10-560}$ concentrations at the sampling site

Table 2 summarizes the BC mass and  $N_{10-560}$  concentrations throughout the sampling period. According to long-term measurement results, the mean BC mass concentrations in the spring, summer, autumn, and winter were  $3.3 \mu\text{g m}^{-3}$ ,  $3.2 \mu\text{g m}^{-3}$ ,  $2.4 \mu\text{g m}^{-3}$ , and  $3.1 \mu\text{g m}^{-3}$ , respectively. The BC mass concentrations did not significantly differ between spring and summer ( $p = 0.070$ ). However, the BC mass concentrations in both spring and summer were significantly higher than those in the winter (all  $p < 0.001$ ). The lowest BC mass concentrations occurred in the autumn among all of the seasons (all  $p < 0.001$ ). Limited information is available on BC mass concentrations in Taipei urban area. Chou et al. (2010) indicated that elemental carbon (EC) mass concentrations in the spring, summer, autumn, and winter were  $3.4 \mu\text{g m}^{-3}$ ,  $3.0 \mu\text{g m}^{-3}$ ,  $2.3 \mu\text{g m}^{-3}$ , and  $2.5 \mu\text{g m}^{-3}$ , respectively, in Taipei urban area from 2003 to 2007. Compared with the measurement results of Chou et al. (2010), the EC mass concentrations and its seasonal variations resembled those in this study. In addition, Cheng et al. (2013) noted that BC mass concentrations were approximately  $3.5 \mu\text{g m}^{-3}$  at a traffic roadside in Taipei urban area.

**Table 1.** Meteorological data at the monitoring site

	Mean <sup>a</sup> (S.D. <sup>b</sup> )	Min–Max <sup>c</sup>	Median	Q <sub>1</sub> –Q <sub>3</sub> <sup>d</sup>
<i>Wind speed, m s<sup>-1</sup></i>				
Spring	1.6 (1.0)	0.0–6.1	1.5	0.8–2.4
Summer	1.3 (1.0)	0.0–6.0	1.0	0.6–1.8
Autumn	1.8 (1.0)	0.0–4.7	1.8	0.9–2.5
Winter	1.6 (1.1)	0.0–10.0	1.5	0.6–2.4
<i>Wind direction<sup>e</sup></i>				
Spring	ENE–ESE			
Summer	ENE–ESE (37%); WNW–WSW (32%)			
Autumn	ENE–ESE			
Winter	ENE–ESE			
<i>Temperature, °C</i>				
Spring	23.1 (4.7)	11.9–39.1	23.0	19.7–26.3
Summer	30.0 (3.4)	18.8–40.5	29.8	27.8–32.3
Autumn	25.7 (3.7)	14.6–37.8	25.6	23.3–28.0
Winter	17.0 (4.2)	5.5–29.9	17.4	14.2–19.6
<i>Relative humidity, %</i>				
Spring	74.7 (12.8)	17.5–98.7	76.1	65.9–84.9
Summer	74.3 (11.3)	41.5–99.0	75.2	65.9–82.7
Autumn	75.6 (10.4)	40.5–98.8	76.7	68.8–83.0
Winter	75.4 (11.3)	38.2–99.0	76.9	67.3–84.3

<sup>a</sup> Observation number  $N = 21\,527$

<sup>b</sup> Standard deviation

<sup>c</sup> Minimal value–maximal value

<sup>d</sup> First quartile value–third quartile value

<sup>e</sup> Prevalent wind direction

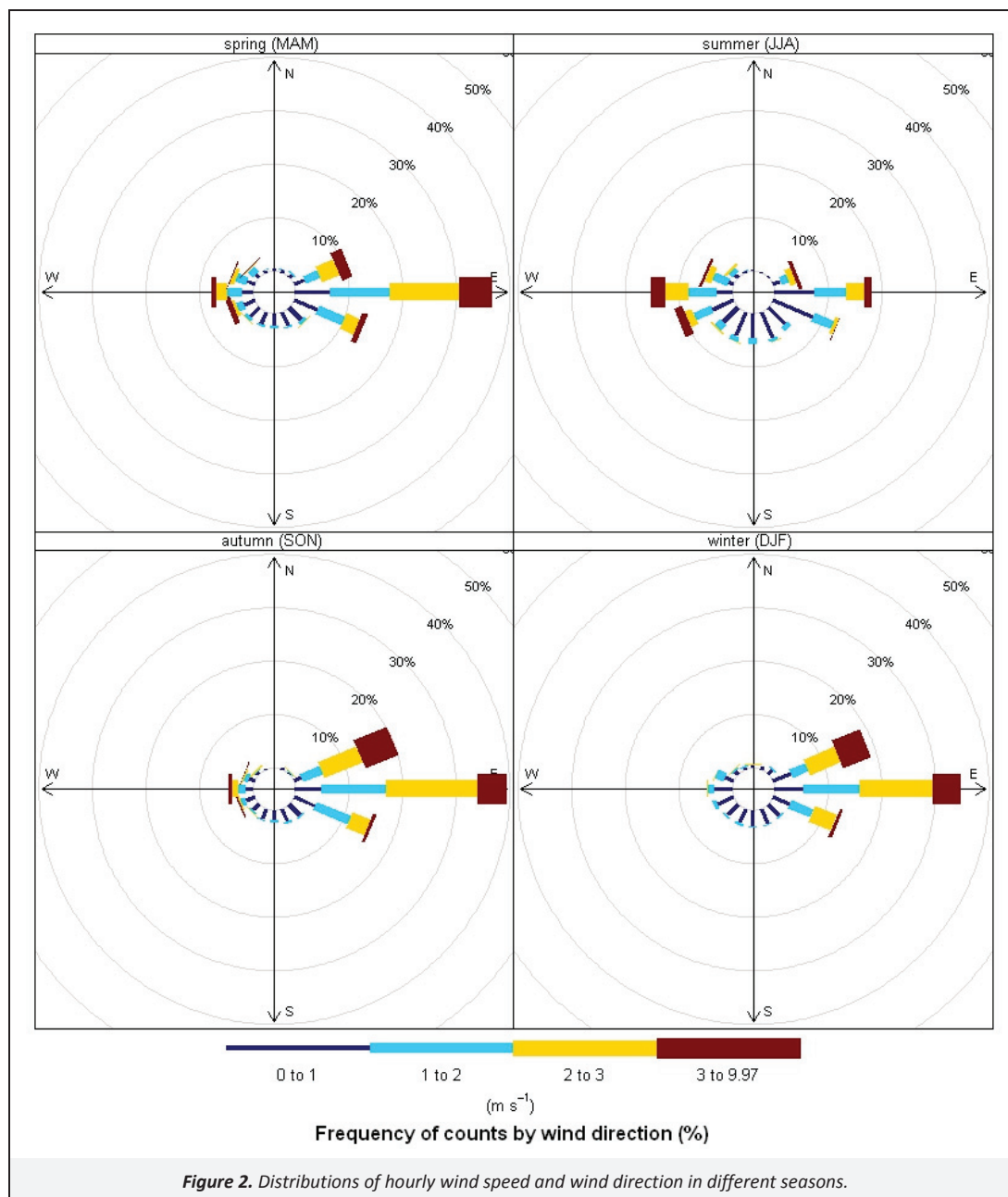


**Table 2.** BC mass and  $N_{10-560}$  concentrations at the monitoring site

	Mean <sup>a</sup> (S.D. <sup>b</sup> )	Min–Max <sup>c</sup>	Median	Q <sub>1</sub> –Q <sub>3</sub> <sup>d</sup>	
		<i>BC, <math>\mu\text{g m}^{-3}</math></i>			
Spring	3.3 (2.3)	0.3–28.3	2.7	1.7–4.1	
Summer	3.2 (1.8)	0.2–36.9	2.9	2.0–4.0	
Autumn	2.4 (1.5)	0.2–13.0	2.0	1.4–2.9	
Winter	3.1 (2.6)	0.2–18.2	2.2	1.4–3.8	
		<i><math>N_{10-560}</math>, particles cm<sup>-3</sup></i>			
Spring	$1.5 \times 10^4$ ( $8.4 \times 10^3$ )	$1.7 \times 10^3$ – $7.2 \times 10^4$	$1.3 \times 10^4$	$8.6 \times 10^3$ – $1.9 \times 10^4$	
Summer	$1.7 \times 10^4$ ( $7.8 \times 10^3$ )	$1.4 \times 10^3$ – $8.0 \times 10^4$	$1.6 \times 10^4$	$1.2 \times 10^4$ – $2.1 \times 10^4$	
Autumn	$1.1 \times 10^4$ ( $5.9 \times 10^3$ )	$1.0 \times 10^3$ – $3.9 \times 10^4$	$1.0 \times 10^4$	$7.1 \times 10^3$ – $1.5 \times 10^4$	
Winter	$1.4 \times 10^4$ ( $1.0 \times 10^4$ )	$1.6 \times 10^3$ – $7.0 \times 10^4$	$1.2 \times 10^4$	$7.6 \times 10^3$ – $1.8 \times 10^4$	

<sup>a</sup> Observation number  $N=21\,527$

<sup>b</sup> Standard deviation

<sup>c</sup> Minimum value–maximum value

<sup>d</sup> First quartile value–third quartile value

However, the BC concentrations at other places could be lower or higher than those in this study, owing to their different meteorological conditions and various emission strengths. Venkatachari et al. (2006) noted that the BC mass concentrations were 1.1–1.4  $\mu\text{g m}^{-3}$  at two sites in New York City. Perez et al. (2010) demonstrated that BC mass concentrations were approximately 3.6  $\mu\text{g m}^{-3}$  and their variability was obviously influenced by traffic emissions in urban Barcelona, Spain. Boogaard et al. (2011) found that BC mass concentrations on major streets in five Dutch cities were 2.1–4.4  $\mu\text{g m}^{-3}$  and approximately 1.5–2.2 times higher than those at urban background locations. Moreover, Begum et al. (2012) demonstrated that BC mass concentrations could reach as high as 22.8  $\mu\text{g m}^{-3}$  in Dhaka, Bangladesh, suggesting that local sources of BC were traffic, coal, and biomass burning. Additionally, Reddy et al. (2012) noted that BC mass concentrations were approximately 3.0  $\mu\text{g m}^{-3}$  in Anantapur, Southeast India, suggesting that local sources and meteorology governed BC concentrations. Sharma et al. (2012) showed that BC mass concentrations were significantly varied monthly between 3.0  $\mu\text{g m}^{-3}$  and 14.9  $\mu\text{g m}^{-3}$  in Kathmandu, Nepal, and the highest BC concentration occurred during winter and pre-monsoon seasons.

According to long-term measurement results, the  $N_{10-560}$  concentrations in the spring, summer, autumn, and winter were  $1.5 \times 10^4$  particles  $\text{cm}^{-3}$ ,  $1.7 \times 10^4$  particles  $\text{cm}^{-3}$ ,  $1.1 \times 10^4$  particles  $\text{cm}^{-3}$ , and  $1.4 \times 10^4$  particles  $\text{cm}^{-3}$ , respectively. The highest and lowest average  $N_{10-560}$  concentrations were observed in the summer (all  $p < 0.001$ ) and autumn (all  $p < 0.001$ ), respectively, at this sampling site. Additionally, the average  $N_{10-560}$  concentrations did not significantly differ between spring and winter ( $p = 0.161$ ). Concentrations of particle numbers evaluated in this site were similar to those measured in other urban areas and were in the range of  $1.0 \times 10^4$ – $2.0 \times 10^4$  particles  $\text{cm}^{-3}$ . Tuch et al. (1997), Ruuskanen et al. (2001) and Pekkanen et al. (2002) noted that outdoor ambient particle number concentrations in eastern Germany, in three European cities, and in Helsinki were  $1.31 \times 10^4$  particles  $\text{cm}^{-3}$ ,  $1.62 \times 10^4$ – $1.83 \times 10^4$  particles  $\text{cm}^{-3}$ , and  $1.49 \times 10^4$  particles  $\text{cm}^{-3}$ , respectively. Additionally, Rodriguez et al. (2007) obtained similar results, indicating that particle number concentrations in Milan, Barcelona and London were  $2.06 \times 10^4$  particles  $\text{cm}^{-3}$ ,  $1.44 \times 10^4$  particles  $\text{cm}^{-3}$  and  $9.33 \times 10^3$  particles  $\text{cm}^{-3}$ , respectively. Gao et al. (2007) demonstrated that particle number concentrations in the summer and winter were  $1.03 \times 10^4$  particles  $\text{cm}^{-3}$  and  $1.56 \times 10^4$  particles  $\text{cm}^{-3}$ , respectively, in Ji'nan, China. Moreover, Gao et al. (2009) noted that particle number concentrations were  $2.85 \times 10^4$  particles  $\text{cm}^{-3}$  in Taicang, China. However, differences in particle number concentrations among these monitoring sites may be due to different monitoring conditions such as measurement time, place, season and equipment. For example, the particle number concentrations presented in previous studies could be measured in different size ranges with different monitoring instruments. In the Taipei urban area, the particle number concentrations at the traffic roadside and highway toll station were  $2.0 \times 10^4$  and  $6.5 \times 10^4$  particles  $\text{cm}^{-3}$ , respectively, and higher than those in this study (Cheng et al., 2010a; Cheng et al. 2013). Moreover, the particle number concentrations could be high as  $> 1.0 \times 10^6$  particles  $\text{cm}^{-3}$  inside the highway tunnel in the Taipei urban area (Cheng et al., 2010b).

The reduced levels of BC mass and particle number in the autumn in this study was mostly likely attributed to the high wind speed conditions that favored horizontal dispersion. Additionally, the highest particle number concentrations in summer could be owing to that more particles were generated from photochemical nucleation processes under the higher solar radiation (or temperature) occurred in the summer compared to that in other seasons.

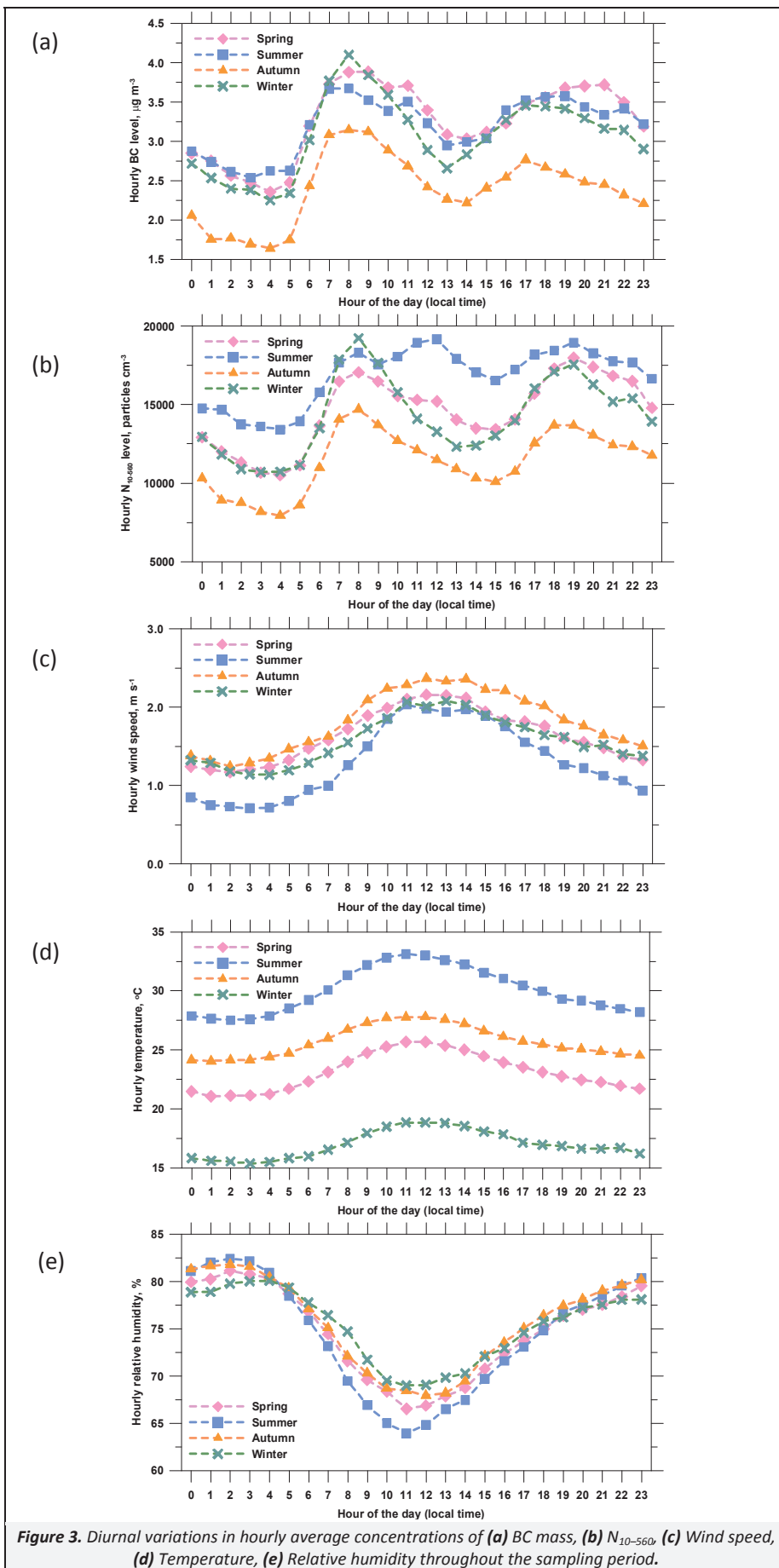
Figure 3a–3e presents diurnal variations in hourly average BC mass,  $N_{10-560}$ , wind speed, temperature and relative humidity throughout the sampling period. In spite of the diurnal variations

of  $N_{10-560}$  concentrations in the summer, the diurnal variations in hourly average BC mass concentrations were similar to those of the  $N_{10-560}$  concentrations in the spring, autumn and winter. Long-term measurement results indicate that BC mass and  $N_{10-560}$  concentrations peaked during the morning (7:00–9:00) and evening (18:00–20:00) rush hours. Additionally, low BC mass and  $N_{10-560}$  concentrations existed in the early morning (1:00–5:00) and afternoon (13:00–14:00) could be likely attributed to the low traffic emission and high wind speed (Figure 3c), respectively, at these two periods. However, a peak of the particle number concentration at midday was observed in the summer (Figure 3b). In summer, the elevated particle number concentration at midday may be attributed to that particle nucleation likely occurred at a high temperature condition (that will be discussed in the next section). Pey et al. (2008), Perez et al. (2010), Cheung et al. (2011) and Reche et al. (2011) noted that particle number concentrations could be enhanced due to the formation of secondary particles in the atmosphere by photochemical nucleation under high solar radiation intensity. During the whole sampling period, the average temperature at noontime was high as 33 °C at the monitoring site in the summer seasons (Figure 3d). That is why the high particle number concentrations could be observed in the summer in this study compared to those in other seasons.

### 3.3. Diurnal variations in particle number size distributions

Particle number size distributions in the Taipei urban area are seldom reported. Figure 4a–4d shows diurnal variations in particle number size distributions, as measured in different seasons. Long-term measurement results indicate that the mode diameter ( $D_m$ ) of particles during the daytime was significantly smaller than that during the early morning hours. The mode diameter of particles was smallest at the initial stage of the morning and evening rush hours, indicating that most particles during these periods were relatively fresh and related to traffic emissions. Following the rush hours, the mode diameter increased and the particle number decreased, likely owing to the coagulation of particles, especially under high particle number concentration conditions. In summer, the new formation of particles was also observed during the period 10:00–14:00 throughout the photochemical nucleation process. During this process, the mode diameter of particles decreased at the initial stage when new small particles were generated from photochemical nucleation, following by an increase in the mode diameter of particles due to the subsequent coagulation. Pey et al. (2008) and Gao et al. (2012) attributed the elevated particle number concentrations at noontime to the new particle formation promoted by photochemical nucleation. Additionally, a larger mode diameter of particles in the early morning hours than during the daytime was likely due to condensation or coagulation of particles under low temperatures and high relative humidity in the early morning hours in this study (Figure 3d–3e). Based on long-term observations, the largest mode diameter of particles during both daytime and early morning hours was observed in the same season (summer). Formation of a larger mode diameter of particles by nucleation and coagulation resulted due to the existence of particles in higher concentrations in the summer than in the other seasons.

Shi et al. (1999) demonstrated that the 24-h average particle number mode diameters on a busy roadside, 30 m from the busy road and 100 m from the busy road, in Birmingham were about 20–30 nm, 30 nm and 30–40 nm, respectively. Rodriguez et al. (2007) determined that the hourly average particle number mode diameters were 36–38 nm in three urban areas in Barcelona, Spain, London, England, and Milan, Italy. Cheng et al. (2013) noted that the hourly average particle number mode diameter was 44 nm at a heavy traffic roadside in Taipei urban area. Mode diameter of the particle number measured in this study was larger than that obtained by Shi et al. (1999), Rodriguez et al. (2007) and Cheng et al. (2013) may be due to that Taipei Aerosol Supersite is located in a sports park and the eastern part (upwind) of this site is a



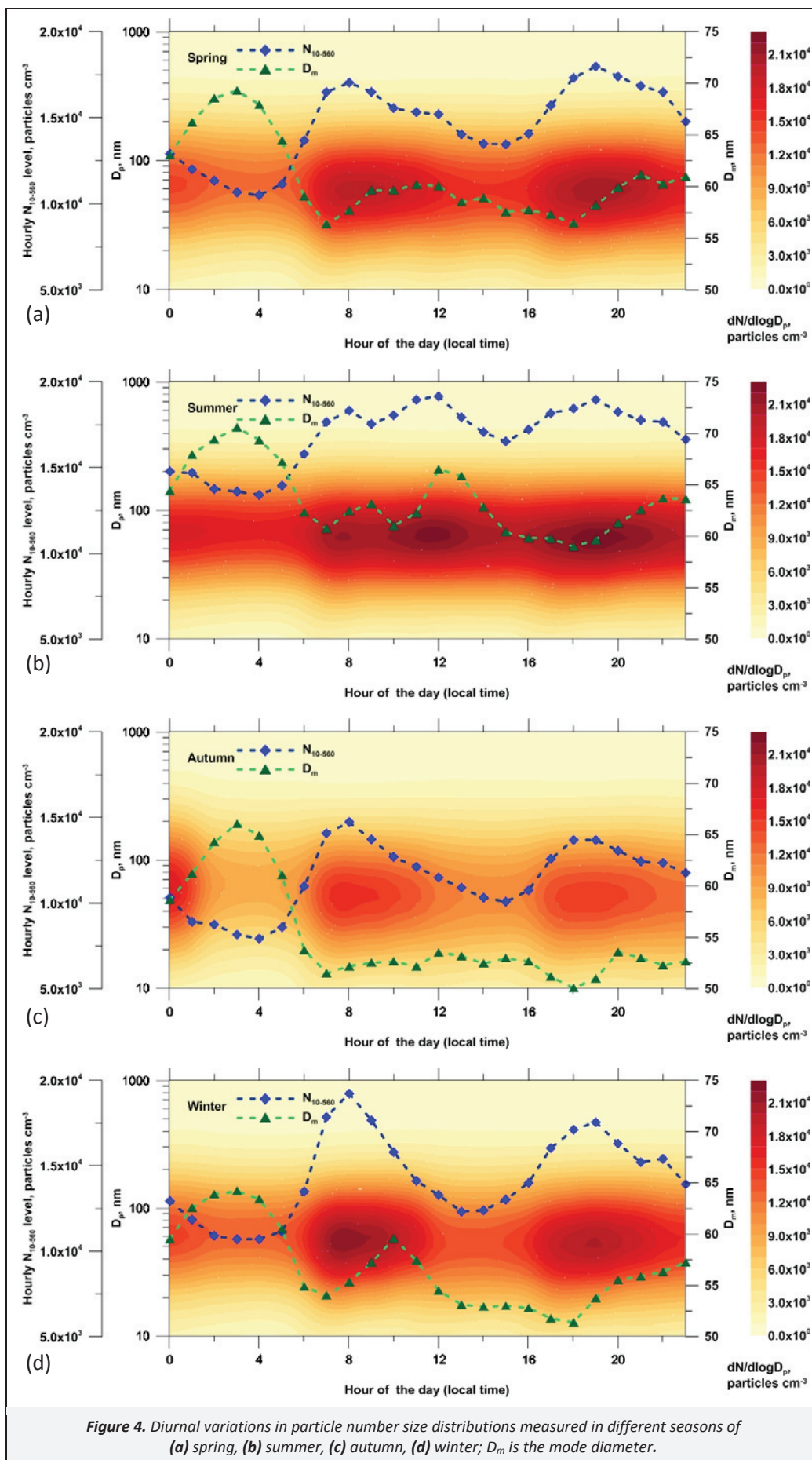


Figure 4. Diurnal variations in particle number size distributions measured in different seasons of (a) spring, (b) summer, (c) autumn, (d) winter;  $D_m$  is the mode diameter.

residential and commercial area, not a major traffic area. The distance between the sampling site and the upwind traffic road is approximately 350 m. The particles in the atmosphere could be grown through coagulation process before they were measured at this sampling site.

#### 3.4. Seasonal variation in the correlation between BC mass and size-selected particle number concentrations

Little information is available on the correlation between BC mass concentrations and size-selected particle number concentrations. Table 3 presents the correlations between BC mass concentrations and particle number concentrations in seven selected size ranges. In this sampling site, the number fractions for  $N_{10-18}$ ,  $N_{18-32}$ ,  $N_{32-56}$ ,  $N_{56-100}$ ,  $N_{100-180}$ ,  $N_{180-320}$  and  $N_{320-560}$  were 4.39%, 15.38%, 26.31%, 27.35%, 16.89%, 7.17% and 2.51%, respectively. Measurement results suggest that the mean particle number concentrations over these seven selected fractions were governed by particles in the size range of 32–100 nm. According to long-term measurement results, hourly BC mass concentrations were significantly positively correlated with hourly  $N_{100-180}$  concentrations at the sampling site ( $R_{pearson}=0.743$ ,  $p<0.001$ ), followed by hourly  $N_{180-320}$  concentrations ( $R_{pearson}=0.716$ ,  $p<0.001$ ) and hourly  $N_{56-100}$  concentrations ( $R_{pearson}=0.689$ ,  $p<0.001$ ). A negative (or low) correlation between hourly BC mass concentrations and hourly  $N_{10-18}$  levels (or  $N_{18-32}$  levels) could be attributed to the highly variable particle number concentrations during sampling. Particles in a size range <32 nm could be grown rapidly through gas-to-particle reactions or coagulations in the atmosphere. Based on measurement results, the correlations between hourly BC mass concentrations and size resolved particle number concentrations in the summer were significantly lower than those in other seasons, indicating that the sources of particles in the summer were not exactly same as those in other seasons. Therefore, a significant amount of particles in the summer could be generated through photochemical nucleation.

Additionally, long-term measurement results indicate that most of the BC in aerosols in Taipei urban area could range from 100–180 nm in size. Unfortunately, there are not any mass size distribution data of BC to verify it. Rodriguez et al. (2008) and Reche et al. (2011) demonstrated that BC mass concentrations in an urban area were positively correlated with particle number concentrations ranging from 3–1 000 nm. Compared with measurements of Rodriguez et al. (2008) and Reche et al. (2011), BC mass concentrations in this study were more strongly correlated with particle number concentrations in a range of 100–180 nm than those acquired in Rodriguez et al. (2008) and Reche et al. (2011). Moreover, Park et al. (2006) acquired similar results, indicating that BC mass concentrations were positively associated with particle number concentrations ranging from 84–407 nm, regardless of the season. Cheng et al. (2013) also demonstrated that BC mass concentrations were positively associated with particle number concentrations ranging from 56–180 nm, which were measured at a heavy traffic roadside. The difference in these studies may be

resulted from the variations in the particle size distributions during the sampling periods in different sampling locations.

Figure 5a–5d shows the daily variations of the  $N_i/BC$  ratios in various particle size ranges, where  $i$  is the selected size range. Except for the summer, the daily evolutions of the  $N_i/BC$  ratios in these seven selected size ranges were similar. In the summer, a clear increase in  $N_{10-560}/BC$  was observed during the noontime period, coincident with maximum ambient temperature (Figure 3d). This peak in particle number concentrations was probably caused by photochemical nucleation processes. A similar result was acquired by the Perez et al. (2010). In this study, the  $N_i/BC$  ratios were significantly elevated in the size range of 32–180 nm during the noontime period in the summer compared to other particle size ranges, suggesting that secondary particles through the photochemical nucleation heavily impacted the size range of 56–100 nm (Figure 5b), following by 100–180 nm (Figure 5c) and 32–56 nm (Figure 5a). Additionally, the daily evolutions of the  $N_i/BC$  ratios in the size range of 56–100 nm and 100–180 nm in the summer were significantly higher than those in other seasons for the whole day. These measurement results indicate that the activities of the chemical nucleation and gas-to-particle reactions in the summer were more intense than those in other seasons.

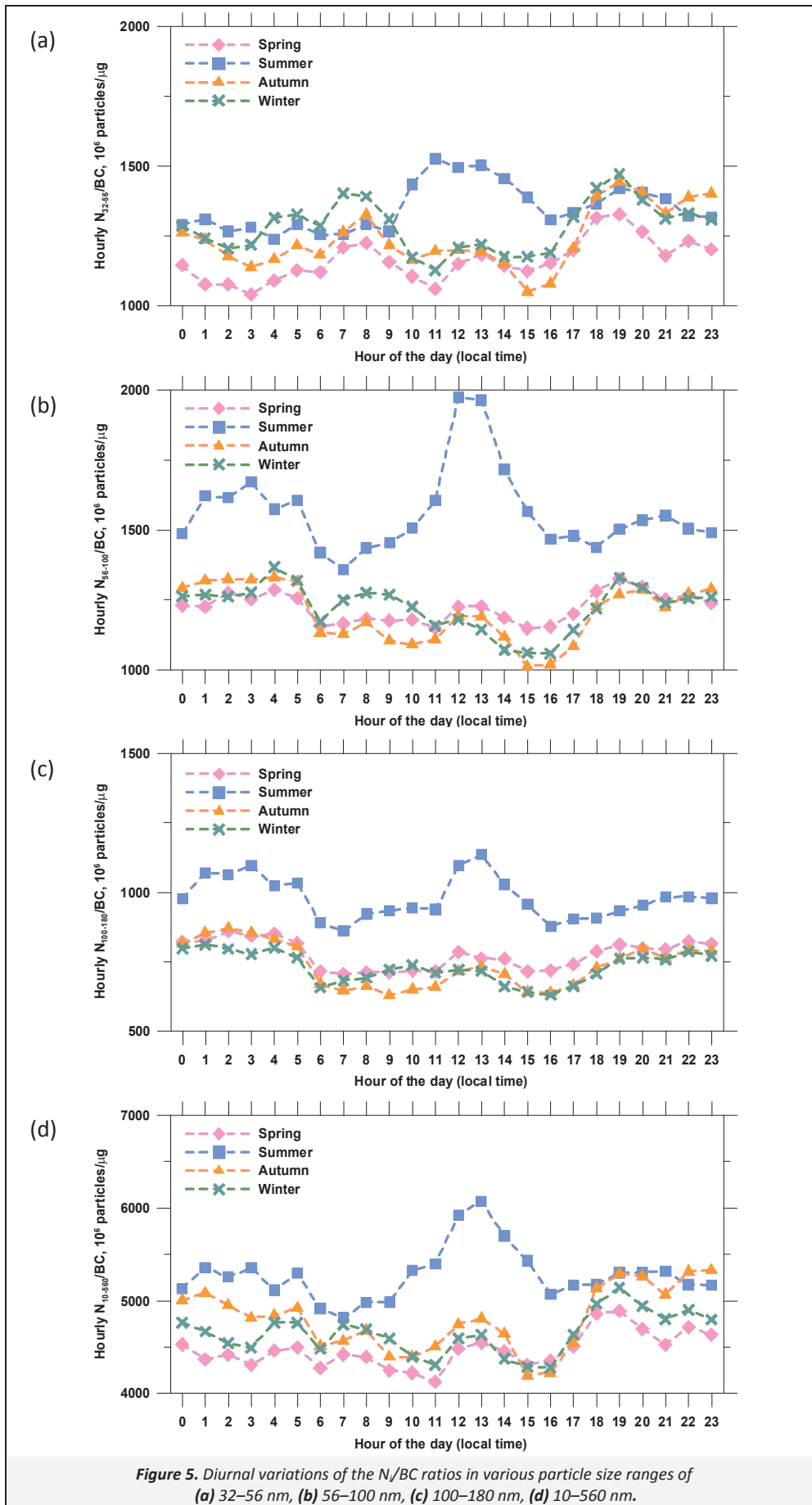
#### 4. Conclusions

Long-term measurement results of this study demonstrate that BC mass concentrations in the spring, summer, autumn, and winter are  $3.3 \mu\text{g m}^{-3}$ ,  $3.2 \mu\text{g m}^{-3}$ ,  $2.4 \mu\text{g m}^{-3}$ , and  $3.1 \mu\text{g m}^{-3}$ , respectively. Additionally, the  $N_{10-560}$  concentrations in the spring, summer, autumn, and winter are  $1.5 \times 10^4$  particles  $\text{cm}^{-3}$ ,  $1.7 \times 10^4$  particles  $\text{cm}^{-3}$ ,  $1.1 \times 10^4$  particles  $\text{cm}^{-3}$ , and  $1.4 \times 10^4$  particles  $\text{cm}^{-3}$ , respectively. In the autumn, the lowest BC mass and particle number concentrations are most likely owing to the high wind speed condition that favored dispersion of particulate matter. Additionally, the highest particle number concentrations observed in the summer can be due to that the activities of the chemical nucleation and gas-to-particle reactions in the summer are more intense than those in other seasons. In this sampling site, the number fractions for  $N_{10-18}$ ,  $N_{18-32}$ ,  $N_{32-56}$ ,  $N_{56-100}$ ,  $N_{100-180}$ ,  $N_{180-320}$  and  $N_{320-560}$  are 4.39%, 15.38%, 26.31%, 27.35%, 16.89%, 7.17% and 2.51%, respectively. Hourly BC mass concentrations are significantly positively correlated with hourly  $N_{100-180}$  concentrations at the sampling site. In the summer, a clear increase in  $N_{10-560}/BC$  is observed during the noontime period, coincident with maximum ambient temperature. Secondary particles through the photochemical nucleation heavily impact the size range of 56–100 nm, following by 100–180 nm and 32–56 nm in this study. In urban areas, BC is a subject of interest for various reasons, one of which is that it causes harmful environmental and health effects. Therefore, it is an interesting issue in further investigations to demonstrate that most BC in aerosols in urban areas is in the submicron size range. Additionally, how to reduce the levels of particles in the submicron size range also can be an important issue to cut down the levels of BC in the atmosphere.

**Table 3.** Pearson correlation coefficients between BC mass and particle number concentrations in seven selected size ranges at the monitoring site.

	$N_{10-18}$	$N_{18-32}$	$N_{32-56}$	$N_{56-100}$	$N_{100-180}$	$N_{180-320}$	$N_{320-560}$	$N_{10-560}$
Spring	-0.089	0.214	0.597	0.742	0.798	0.765	0.640	0.734
Summer	-0.150	0.050	0.338	0.505	0.595	0.559	0.291	0.500
Autumn	-0.061	0.250	0.588	0.687	0.754	0.722	0.553	0.696
Winter	-0.075	0.285	0.648	0.770	0.806	0.778	0.753	0.761
Overall	-0.100	0.201	0.556	0.689	0.743	0.716	0.523	0.689

All  $p<0.001$



## Acknowledgments

The authors would like to thank the National Science Council of the Republic of China, Taiwan, for financially supporting this research under Contract No. NSC101–2221–E–131–026. The Environmental Protection Administration of the Republic of China, Taiwan, is commended for providing the long-term measurement data.

## References

- Beckerman, B., Jerrett, M., Brook, J.R., Verma, D.K., Arain, M.A., Finkelstein, M.M., 2008. Correlation of nitrogen dioxide with other traffic pollutants near a major expressway. *Atmospheric Environment* 42, 275–290.
- Begum, B.A., Hossain, A., Nahar, N., Markwitz, A., Hopke, P.K., 2012. Organic and black carbon in PM<sub>2.5</sub> at an urban site at Dhaka, Bangladesh. *Aerosol and Air Quality Research* 12, 1062–1072.
- Bond, T.C., Doherty, S.J., Fahey, D.W., Forster, P.M., Berntsen, T., DeAngelo, B.J., Flanner, M.G., Ghan, S., Karcher, B., Koch, D., Kinne, S., Kondo, Y., Quinn, P.K., Sarofim, M.C., Schultz, M.G., Schulz, M., Venkataraman, C., Zhang, H., Zhang, S., Bellouin, N., Guttikunda, S.K., Hopke, P.K., Jacobson, M.Z., Kaiser, J.W., Klimont, Z., Lohmann, U., Schwarz, J.P., Shindell, D., Storelvmo, T., Warren, S.G., Zender, C.S., 2013. Bounding the role of black carbon in the climate system: A scientific assessment. *Journal of Geophysical Research–Atmospheres* 118, 5380–5552.
- Boogaard, H., Kos, G.P.A., Weijers, E.P., Janssen, N.A.H., Fischer, P.H., van der Zee, S.C., de Hartog, J.J., Hoek, G., 2011. Contrast in air pollution components between major streets and background locations: Particulate matter mass, black carbon, elemental composition, nitrogen oxide and ultrafine particle number. *Atmospheric Environment* 45, 650–658.
- Chang, S.Y., Lee, C.T., Chou, C.C.K., Liu, S.C., Wen, T.X., 2007. The continuous field measurements of soluble aerosol compositions at the Taipei Aerosol Supersite, Taiwan. *Atmospheric Environment* 41, 1936–1949.
- Cheng, Y.H., Shiu, B.T., Lin, M.H., Yan, J.W., 2013. Levels of black carbon and their relationship with particle number levels—observation at an urban roadside in Taipei City. *Environmental Science and Pollution Research* 20, 1537–1545.
- Cheng, Y.H., Huang, C.H., Huang, H.L., Tsai, C.J., 2010a. Concentrations of ultrafine particles at a highway toll collection booth and exposure implications for toll collectors. *Science of the Total Environment* 409, 364–369.
- Cheng, Y.H., Liu, Z.S., Chen, C.C., 2010b. On-road measurements of ultrafine particle concentration profiles and their size distributions inside the longest highway tunnel in Southeast Asia. *Atmospheric Environment* 44, 763–772.
- Cheung, H.C., Morawska, L., Ristovski, Z.D., 2011. Observation of new particle formation in subtropical urban environment. *Atmospheric Chemistry and Physics* 11, 3823–3833.
- Chou, C.C.K., Lee, C.T., Cheng, M.T., Yuan, C.S., Chen, S.J., Wu, Y.L., Hsu, W.C., Lung, S.C., Hsu, S.C., Lin, C.Y., Liu, S.C., 2010. Seasonal variation and spatial distribution of carbonaceous aerosols in Taiwan. *Atmospheric Chemistry and Physics* 10, 9563–9578.
- Donaldson, K., Brown, D., Clouter, A., Duffin, R., MacNee, W., Renwick, L., Tran, L., Stone, V., 2002. The pulmonary toxicology of ultrafine particles. *Journal of Aerosol Medicine–Deposition Clearance and Effects in the Lung* 15, 213–220.
- Duhme, H., Weiland, S.K., Keil, U., 1998. Epidemiological analyses of the relationship between environmental pollution and asthma. *Toxicology Letters* 103, 307–316.
- Fruin, S., Westerdaahl, D., Sax, T., Sioutas, C., Fine, P.M., 2008. Measurements and predictors of on-road ultrafine particle concentrations and associated pollutants in Los Angeles. *Atmospheric Environment* 42, 207–219.
- Gao, J., Chai, F.H., Wang, T., Wang, S.L., Wang, W.X., 2012. Particle number size distribution and new particle formation: New characteristics during the special pollution control period in Beijing. *Journal of Environmental Sciences–China* 24, 14–21.
- Gao, J., Wang, T., Zhou, X.H., Wu, W.S., Wang, W.X., 2009. Measurement of aerosol number size distributions in the Yangtze River delta in China: Formation and growth of particles under polluted conditions. *Atmospheric Environment* 43, 829–836.
- Gao, J., Wang, J., Cheng, S.H., Xue, L.K., Yan, H.Z., Hou, L.J., Jiang, Y.Q., Wang, W.X., 2007. Number concentration and size distributions of submicron particles in Jinan urban area: Characteristics in summer and winter. *Journal of Environmental Sciences–China* 19, 1466–1473.
- Gilmour, P.S., Ziesenis, A., Morrison, E.R., Vickers, M.A., Drost, E.M., Ford, I., Karg, E., Mossa, C., Schroepel, A., Ferron, G.A., Heyder, J., Greaves, M., MacNee, W., Donaldson, K., 2004. Pulmonary and systemic effects of short-term inhalation exposure to ultrafine carbon black particles. *Toxicology and Applied Pharmacology* 195, 35–44.
- Hagler, G.S.W., Baldauf, R.W., Thoma, E.D., Long, T.R., Snow, R.F., Kinsey, J.S., Oudejans, L., Gullett, B.K., 2009. Ultrafine particles near a major roadway in Raleigh, North Carolina: Downwind attenuation and correlation with traffic-related pollutants. *Atmospheric Environment* 43, 1229–1234.
- Harrison, R.M., Jones, A.M., Lawrence, R.G., 2004. Major component composition of PM<sub>10</sub> and PM<sub>2.5</sub> from roadside and urban background sites. *Atmospheric Environment* 38, 4531–4538.
- Hussein, T., Hameri, K.A., Aalto, P.P., Paatero, P., Kulmala, M., 2005. Modal structure and spatial-temporal variations of urban and suburban aerosols in Helsinki – Finland. *Atmospheric Environment* 39, 1655–1668.
- Hussein, T., Puustinen, A., Aalto, P.P., Makela, J.M., Hameri, K., Kulmala, M., 2004. Urban aerosol number size distributions. *Atmospheric Chemistry and Physics* 4, 391–411.
- Invernizzi, G., Ruprecht, A., Mazza, R., De Marco, C., Mocnik, G., Sioutas, C., Westerdaahl, D., 2011. Measurement of black carbon concentration as an indicator of air quality benefits of traffic restriction policies within the ecopass zone in Milan, Italy. *Atmospheric Environment* 45, 3522–3527.
- Jacobson, M.Z., 2010. Short-term effects of controlling fossil-fuel soot, biofuel soot and gases, and methane on climate, Arctic ice, and air pollution health. *Journal of Geophysical Research–Atmospheres* 115, art. no. D14209.
- Jansen, K.L., Larson, T.V., Koenig, J.Q., Mar, T.F., Fields, C., Stewart, J., Lippmann, M., 2005. Associations between health effects and particulate matter and black carbon in subjects with respiratory disease. *Environmental Health Perspectives* 113, 1741–1746.
- Kondo, Y., Sahu, L., Moteki, N., Khan, F., Takegawa, N., Liu, X., Koike, M., Miyakawa, T., 2011. Consistency and traceability of black carbon measurements made by laser-induced incandescence, thermal-optical transmittance, and filter-based photo-absorption techniques. *Aerosol Science and Technology* 45, 295–312.
- Matson, U., 2005. Indoor and outdoor concentrations of ultrafine particles in some Scandinavian rural and urban areas. *Science of the Total Environment* 343, 169–176.
- Morawska, L., Ristovski, Z., Jayaratne, E.R., Keogh, D.U., Ling, X., 2008. Ambient nano and ultrafine particles from motor vehicle emissions: Characteristics, ambient processing and implications on human exposure. *Atmospheric Environment* 42, 8113–8138.
- Oberdorster, G., Sharp, Z., Atudorei, V., Elder, A., Gelein, R., Lunts, A., Kreyling, W., Cox, C., 2002. Extrapulmonary translocation of ultrafine carbon particles following whole-body inhalation exposure of rats. *Journal of Toxicology and Environmental Health–Part A* 65, 1531–1543.
- Park, K., Chow, J.C., Watson, J.G., Trimble, D.L., Doraiswamy, P., Park, K., Arnott, W.P., Stroud, K.R., Bowers, K., Bode, R., Petzold, A., Hansen, A.D.A., 2006. Comparison of continuous and filter-based carbon measurements at the Fresno Supersite. *Journal of the Air & Waste Management Association* 56, 474–491.

- Pekkanen, J., Peters, A., Hoek, G., Tiittanen, P., Brunekreef, B., de Hartog, J., Heinrich, J., Ibalá-Mulli, A., Kreyling, W.G., Lanki, T., Timonen, K.L., Vanninen, E., 2002. Particulate air pollution and risk of ST-segment depression during repeated submaximal exercise tests among subjects with coronary heart disease – the Exposure and Risk Assessment for Fine and Ultrafine Particles in Ambient Air (ULTRA) study. *Circulation* 106, 933–938.
- Perez, N., Pey, J., Cusack, M., Reche, C., Querol, X., Alastuey, A., Viana, M., 2010. Variability of particle number, black carbon, and PM<sub>10</sub>, PM<sub>2.5</sub>, and PM<sub>1</sub> levels and speciation: Influence of road traffic emissions on urban air quality. *Aerosol Science and Technology* 44, 487–499.
- Pey, J., Querol, X., Alastuey, A., Rodriguez, S., Putaud, J.P., Van Dingenen, R., 2009. Source apportionment of urban fine and ultra-fine particle number concentration in a Western Mediterranean city. *Atmospheric Environment* 43, 4407–4415.
- Pey, J., Rodriguez, S., Querol, X., Alastuey, A., Moreno, T., Putaud, J.P., Van Dingenen, R., 2008. Variations of urban aerosols in the Western Mediterranean. *Atmospheric Environment* 42, 9052–9062.
- Pope, C.A., Burnett, R.T., Thurston, G.D., Thun, M.J., Calle, E.E., Krewski, D., Godleski, J.J., 2004. Cardiovascular mortality and long-term exposure to particulate air pollution – Epidemiological evidence of general pathophysiological pathways of disease. *Circulation* 109, 71–77.
- Power, M.C., Weisskopf, M.G., Alexeeff, S.E., Coull, B.A., Spiro, A., Schwartz, J., 2011. Traffic-related air pollution and cognitive function in a cohort of older men. *Environmental Health Perspectives* 119, 682–687.
- Ramanathan, V., Carmichael, G., 2008. Global and regional climate changes due to black carbon. *Nature Geoscience* 1, 221–227.
- Rattigan, O.V., Civerolo, K., Doraiswamy, P., Felton, H.D., Hopke, P.K., 2013. Long term black carbon measurements at two urban locations in New York. *Aerosol and Air Quality Research* 13, 1181–U1305.
- Reche, C., Querol, X., Alastuey, A., Viana, M., Pey, J., Moreno, T., Rodriguez, S., Gonzalez, Y., Fernandez-Camacho, R., de la Campa, A.M.S., de la Rosa, J., Dall'Osto, M., Prevot, A.S.H., Hueglin, C., Harrison, R.M., Quincey, P., 2011. New considerations for PM, black carbon and particle number concentration for air quality monitoring across different European cities. *Atmospheric Chemistry and Physics* 11, 6207–6227.
- Reddy, B.S.K., Kumar, K.R., Balakrishnaiah, G., Gopal, K.R., Reddy, R.R., Reddy, L.S.S., Ahammed, Y.N., Narasimhulu, K., Moorthy, K.K., Babu, S.S., 2012. Potential source regions contributing to seasonal variations of black carbon aerosols over Anantapur in Southeast India. *Aerosol and Air Quality Research* 12, 344–358.
- Rich, D.Q., Schwartz, J., Mittleman, M.A., Link, M., Luttmann-Gibson, H., Catalano, P.J., Speizer, F.E., Dockery, D.W., 2005. Association of short-term ambient air pollution concentrations and ventricular arrhythmias. *American Journal of Epidemiology* 161, 1123–1132.
- Rodriguez, S., Cuevas, E., Gonzalez, Y., Ramos, R., Romero, P.M., Perez, N., Querol, X., Alastuey, A., 2008. Influence of sea breeze circulation and road traffic emissions on the relationship between particle number, black carbon, PM<sub>1</sub>, PM<sub>2.5</sub> and PM<sub>2.5-10</sub> concentrations in a coastal city. *Atmospheric Environment* 42, 6523–6534.
- Rodriguez, S., Cuevas, E., 2007. The contributions of “minimum primary emissions” and “new particle formation enhancements” to the particle number concentration in urban air. *Journal of Aerosol Science* 38, 1207–1219.
- Rodriguez, S., Van Dingenen, R., Putaud, J.P., Dell'Acqua, A., Pey, J., Querol, X., Alastuey, A., Chenery, S., Ho, K.F., Harrison, R.M., Tardivo, R., Scarnato, B., Gemelli, V., 2007. A study on the relationship between mass concentrations, chemistry and number size distribution of urban fine aerosols in Milan, Barcelona and London. *Atmospheric Chemistry and Physics* 7, 2217–2232.
- Ruuskanen, J., Tuch, T., Ten Brink, H., Peters, A., Khlystov, A., Mirme, A., Kos, G.P.A., Brunekreef, B., Wichmann, H.E., Buzorius, G., Vallius, M., Kreyling, W.G., Pekkanen, J., 2001. Concentrations of ultrafine, fine and PM<sub>2.5</sub> particles in three European cities. *Atmospheric Environment* 35, 3729–3738.
- Sandradewi, J., Prevot, A.S.H., Weingartner, E., Schmidhauser, R., Gysel, M., Baltensperger, U., 2008. A study of wood burning and traffic aerosols in an Alpine valley using a multi-wavelength Aethalometer. *Atmospheric Environment* 42, 101–112.
- Schulz, M., Textor, C., Kinne, S., Balkanski, Y., Bauer, S., Bernsten, T., Berglen, T., Boucher, O., Dentener, F., Guibert, S., Isaksen, I.S.A., Iversen, T., Koch, D., Kirkevåg, A., Liu, X., Montanaro, V., Myhre, G., Penner, J.E., Pitari, G., Reddy, S., Seland, O., Stier, P., Takemura, T., 2006. Radiative forcing by aerosols as derived from the AeroCom present-day and pre-industrial simulations. *Atmospheric Chemistry and Physics* 6, 5225–5246.
- Sharma, R.K., Bhattarai, B.K., Sapkota, B.K., Gewali, M.B., Kjeldstad, B., 2012. Black carbon aerosols variation in Kathmandu Valley, Nepal. *Atmospheric Environment* 63, 282–288.
- Shi, J.P., Khan, A.A., Harrison, R.M., 1999. Measurements of ultrafine particle concentration and size distribution in the urban atmosphere. *Science of the Total Environment* 235, 51–64.
- Smargiassi, A., Baldwin, M., Pilger, C., Dugandzic, R., Brauer, M., 2005. Small-scale spatial variability of particle concentrations and traffic levels in Montreal: A pilot study. *Science of the Total Environment* 338, 243–251.
- Snyder, D.C., Rutter, A.P., Worley, C., Olson, M., Plourde, A., Bader, R.C., Dallmann, T., Schauer, J.J., 2010. Spatial variability of carbonaceous aerosols and associated source tracers in two cities in the Midwestern United States. *Atmospheric Environment* 44, 1597–1608.
- Suglia, S.F., Gryparis, A., Schwartz, J., Wright, R.J., 2008. Association between traffic-related black carbon exposure and lung function among urban women. *Environmental Health Perspectives* 116, 1333–1337.
- Tuch, T., Brand, P., Wichmann, H.E., Heyder, J., 1997. Variation of particle number and mass concentration in various size ranges of ambient aerosols in Eastern Germany. *Atmospheric Environment* 31, 4193–4197.
- Venkatachari, P., Zhou, L.M., Hopke, P.K., Felton, D., Rattigan, O.V., Schwab, J.J., Demerjian, K.L., 2006. Spatial and temporal variability of black carbon in New York City. *Journal of Geophysical Research-Atmospheres* 111, art. no. D10S05.
- Westerdahl, D., Fruin, S., Sax, T., Fine, P.M., Sioutas, C., 2005. Mobile platform measurements of ultrafine particles and associated pollutant concentrations on freeways and residential streets in Los Angeles. *Atmospheric Environment* 39, 3597–3610.